Ecotoxicology and Environmental Safety 288 (2024) 117351

Contents lists available at ScienceDirect

Ecotoxicology and Environmental Safety

journal homepage: www.elsevier.com/locate/ecoenv

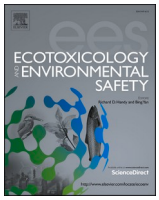

The *Aloe vera* acemannan polysaccharides inhibit phthalate-induced cell viability, metastasis, and stemness in colorectal cancer cells

Pei-Chun Shih [a], Chung-Hsien Lin [a], Uvarani Chokkalingam [c], Ekambaranellore Prakash [c], Ching-Nan Kao [c], Chuan-Fa Chang [a,b,*], Wei-Ling Lin [a,b,*]

[a] Department of Medical Laboratory Science and Biotechnology, National Cheng Kung University, Tainan 70101, Taiwan
[b] Institute of Basic Medical Science, College of Medicine, National Cheng Kung University, Tainan 70101, Taiwan
[c] Dazzeon Biotech Co., Ltd, 248624, Taiwan

ARTICLE INFO

Keywords:
di-ethylhexyl phthalate (DEHP)
mono-ethylhexyl phthalate (MEHP)
Aloe vera
colorectal cancer cell
glycosylation
chemotherapeutic drug resistance

ABSTRACT

Plasticizers are recognized as environmental pollutants that may be associated with a range of health concerns, including impacts on growth, development, and oncogenic risks. Previous research demonstrated that prolonged exposure to di-(2-ethylhexyl) phthalate and its metabolite mono-(2-ethylhexyl) phthalate contributes to chemotherapeutic drug resistance and stemness in colorectal cancer cells. Aloe vera, an herbaceous plant with a long-standing history in traditional medicine, has attracted considerable attention for its diverse pharmacological properties. This study aimed to investigate the therapeutic potential of polysaccharides extracted from Aloe vera, specifically focusing on their anticancer properties. We eluted polysaccharides from Aloe vera using water and ethanol, resulting in the fractions designated A50 and I50, respectively. We characterized their effects on cell viability, migration, invasion, stemness, and glycosylation of colorectal cancer cells exposed to phthalates. Comprehensive glycan analysis revealed that phthalate exposure induced alterations in glycosylation patterns in colorectal cancer cells. Treatment with A50 and I50 reversed these changes to varying degrees, indicating distinct regulatory roles of the two polysaccharide fractions in colorectal cancer cells subjected to phthalate exposure. A50 exhibited a dose-dependent reduction in cell viability induced by phthalates, whereas I50 demonstrated no such effect. Notably, I50 displayed a notable inhibitory effect on migration, invasion, and stemness induced by phthalates when compared with A50. The differing polysaccharide structures of A50 and I50 may account for their divergent effects on the malignancy of colorectal cancer cells. These findings underscore the potential of Aloe vera polysaccharides in anticancer therapy and highlight the necessity for further investigation into their clinical applications.

1. Introduction

Phthalates, mainly utilized as plasticizers in plastics, pose health risks with long-term exposure (Mariana et al., 2023; Winz et al., 2023; Zhang et al., 2022). These chemicals can be released from plastic products and enter the human body through physical contact, inhalation, and liquid absorption. Medical devices, such as polyvinyl chloride plastic bags and tubing sets, frequently contain di(2-ethylhexyl) phthalate (DEHP) (Bernard et al., 2015; Bourdeaux et al., 2016), the most widely used phthalate in plastics. Exposure to DEHP has been associated with resistance to anticancer drugs. DEHP can activate the transcription of the multidrug resistance 1 (MDR1) gene in human colon adenocarcinoma–derived cell lines (Takeshita et al., 2006). Elevated levels of DEHP can induce drug resistance in sarcoma cells by diminishing the cytotoxicity effects of anticancer drugs through increased MDR expression (Angelini et al., 2011). DEHP also mediates drug

Abbreviations: DEHP, Di2-ethylhexyl phthalate; MEHP, Mono-ethylhexyl phthalate; MDR1, multidrug resistance 1; AhR, aryl hydrocarbon receptor; ST8SIA6, alpha-2,8-sialyltransferase 6; HPLC, High-performance liquid chromatography; RID, refractive index detector; UV–vis spectrometry, Ultraviolet-Visible; FT-IR, Fourier-transform infrared; NMR, Nuclear Magnetic Resonance; FBS, fetal bovine serum; CCK-8, Cell Counting Kit-8; LC-MS, liquid chromatography-mass spectrometry; PAG, processed *Aloe vera* gel.

* Correspondence to: Department of Medical Laboratory Science and Biotechnology, College of Medicine, National Cheng Kung University, No 1, University Rd, Tainan City 701, Taiwan.

E-mail addresses: affa@mail.ncku.edu.tw (C.-F. Chang), wling@gs.ncku.edu.tw (W.-L. Lin).

https://doi.org/10.1016/j.ecoenv.2024.117351
Received 11 September 2024; Received in revised form 12 November 2024; Accepted 13 November 2024

resistance in breast cancer by targeting the aryl hydrocarbon receptor (AhR) (Hsieh et al., 2022) and upregulating ATP-binding cassette transporters (Jadhao et al., 2021). Our previous studies demonstrated that exposure of colorectal cancer cells to DEHP or its metabolite mono-ethylhexyl phthalate (MEHP) enhances cell metastasis and resistance to chemotherapeutic drugs by increasing cancer cell stemness (Chen et al., 2018). Furthermore, serum concentrations of DEHP were positively correlated with cancer recurrence. We also found that long-term exposure to DEHP/MEHP induces colorectal cancer cell stemness by altering glycosylation, specifically by reducing alpha-2, 8-sialyltransferase 6 (ST8SIA6) expression (Shih et al., 2023).

Aloe vera, an herbaceous plant utilized for centuries in medicine and food, is esteemed for its anti-inflammatory, antimicrobial, antioxidant, wound-healing, antidiabetic, immunomodulatory, and anti-cancer properties (Balan et al., 2014; Govindarajan et al., 2021; Hekmatpou et al., 2019; Manirakiza et al., 2021; Nejatzadeh-Barandozi, 2013). These benefits arise from its leaf extract, which is rich in bioactive constituents such as polysaccharides, anthraquinones, vitamins, enzymes, and minerals (Maan et al., 2018). Polysaccharides, in particular, play key roles in energy and water storage (Minjares-Fuentes et al., 2018). Comprehensive research has explored the pharmacological properties of *Aloe vera* extract, underscoring its potential applications in the treatment of various health conditions.

Acemannan, the principal bioactive polysaccharide in the gel of *Aloe vera* leaves, consists of O-acetylated mannose chains linked by β-(1,4)-linkages with varying branching and O-acetylation (Ni et al., 2004). This structure contributes to its overall stability and functionality, enabling interaction with various biological molecules and the demonstration of diverse therapeutic properties (Chokboribal et al., 2015; Maan et al., 2018). Primarily, the O-acetyl-groups in acemannan protect cells from hydrogen peroxide induced oxidative damage and facilitate immune functions *in vivo* (Kumar and Kumar, 2019). Conversely, de-O-acetylation negatively impacts acemannan's antibacterial and antibiofilm capabilities (Fatma Salah et al., 2017).

Colorectal cancer ranks among the top in global incidence and mortality (Siegel et al., 2023). Aberrant glycosylation significantly contributes to tumor progression, growth, drug resistance, metastasis, and stemness (Khan and Cabral, 2021; Pinho and Reis, 2015; Very et al., 2018). Acemannan from *Aloe vera* has shown anticancer effects by inhibiting proliferation, promoting apoptosis, and enhancing cytotoxicity in cancer cells, making *Aloe vera* polysaccharides potential anticancer agents (Murtazina et al., 2022; Wang et al., 2023). This study explores the potential of polysaccharides extracted from *Aloe vera* to counteract malignancies from phthalate exposure, specifically DEHP and MEHP. We isolated acemannan from *Aloe vera*, yielding two distinct polysaccharide products, A50 and I50, and subsequently analyzed their structures. Additionally, we examined glycosylation, cell viability, migration, invasion, and stemness in DEHP/MEHP-exposed colorectal cancer cells treated with either A50 or I50.

2. Material and methods

2.1. Extraction, separation, and purification of polysaccharides from Aloe vera gel

Aloe vera lyophilized gel (200:1 concentrate) was prepared from mature leaves of *Aloe vera* supplied by Aloecorp Co., USA., and utilized to isolate *Aloe* polysaccharides. The isolation and purification of these polysaccharides were carried out using a modified protocol previously described (Chokboribal et al., 2015; Tai-Nin Chow et al., 2005). Briefly, Aloe powder was mixed with deionized water and then subjected to the column packed with activated non-polar resin (HP-20 DIAION™, Mitsubishi Chemical Co., Japan). Three fractions were then eluted at a flow rate of 1 L/min using 100 % water, 50 % ethanol, or 100 % ethanol, and the eluents were then freeze-dried. The freeze-dried sample eluted with 100 % water was then mixed with 80 % ethanol to separate the soluble part from the insoluble fibrous (polysaccharide) fraction. Following centrifugation, the precipitate containing polysaccharides was collected and reconstituted with 50 % ethanol for further precipitation. The supernatant was collected and concentrated using a rotary evaporator (Buchi Rotavapor R-220 Pro, Switzerland), and the concentrate was freeze-dried to yield A50. Concurrently, the freeze-dried powder from the 50 % ethanol fraction underwent an 80 % ethanol treatment to obtain I50.

2.2. High-performance liquid chromatography (HPLC)

The acemannan content of *Aloe vera* polysaccharides was determined using HPLC (Agilent 1260 Infinity II, Agilent Technologies Inc., USA). Solutions of *Aloe vera* polysaccharides (A50 and I50) at a concentration of 2.5 mg/mL were prepared in water containing 0.5 % NaN3 (Thermo, USA) by weight. After 8 hours of mixing, the samples were filtered through a 0.2 μm filter and subjected to the chromatographic column. Ultrahydrogel TM 1000 (7.8 × 300 mm, Waters, Japan) and Shodex KS-804 (8 × 300 mm, 1.0 mL/min at 50°C, Japan) columns were used, and the acemannan content of A50 and I50 was detected using a refractive index detector (RID) for HPLC analysis. A calibration curve for quantifying acemannan was established using the acemannan standard.

2.3. Ultraviolet-visible spectrophotometry (UV-Vis spectrophotometry)

The O-acetyl group content of Aloe vera polysaccharides was assessed using a UV–Vis spectrophotometer (Epoch 2, Agilent Technologies Inc., USA). A solution of Aloe vera polysaccharide samples (A50 and I50) at a concentration of 10 mg/mL was prepared. One milliliter of this solution was thoroughly mixed with 2 mL of 2 M hydroxylamine hydrochloride (Sigma, USA). Subsequently, 3.5 M sodium hydroxide (Nippon Shinyaku CO., LTD., Japan) was added, and the mixture was incubated for 4 minutes at room temperature. Following this, 1 mL of 4 M hydrochloric acid (Honeywell International Inc., USA) and a solution of 0.37 M ferric chloride–hydrochloric acid (Sigma, USA) were introduced. The absorbance was measured at 540 nm using the spectrophotometer. An acetylcholine chloride ($C_7H_{16}ClNO_2$, Sigma, USA) solution was utilized to quantify the O-acetyl group content in Aloe vera polysaccharides (Metcalfe, 2019).

2.4. Fourier-transform infrared spectroscopy (FT-IR)

FT-IR was performed to analyze the presence of the O-acetyl group of acemannan from Aloe vera polysaccharides. The freeze-dried powder of A50 and I50 were dissolved in deionized water, and vibrational spectra (500–4000 cm^{-1}) were recorded by using FTIR (Thermo Scientific Nicolet iS5, USA) (Nejatzadeh-Barandozi and Enferadi, 2012; Shi et al., 2018).

2.5. ^{1}H-nuclear magnetic resonance (^{1}H NMR) and ^{13}C-nuclear magnetic resonance (^{13}C NMR)

The ^{1}H NMR and ^{13}C NMR spectra were acquired using a Bruker AVANCE III HD 600 MHz spectrometer equipped with a BBFO probe. The freeze-dried powder of A50 and I50 was dissolved in 99.9 % deuterium oxide (Sigma, USA) and subsequently loaded into Wildman Economic 5 mm NMR tubes. The NMR spectra were analyzed using MestReNova software (version 14.3), with tetramethylsilane employed as an internal standard (Minjares-Fuentes et al., 2017; Shi et al., 2018; Tai-Nin Chow et al., 2005).

2.6. Purification and characterization of N-Glycome

A total of 10^7 cells were suspended in TX-100 extraction buffer and subjected to sonication. The resulting samples were then centrifuged at 13,000 rpm for a duration of 10 minutes, after which the pellets were

discarded. The supernatant underwent treatment with 10 mM dithiothreitol at 37°C for 1 hour, followed by incubation with 50 mM iodoacetamide at 37°C for an additional hour. Subsequently, 10 % trichloroacetic acid was added to each sample and incubated at −20°C for 30 minutes. Following another centrifugation at 13,000 rpm for 10 minutes, the supernatant was discarded, and the resulting pellets were washed twice with acetone. The samples were then subjected to sequential incubation with trypsin, chymotrypsin, and PNGase F to facilitate the cleavage of glycans. N-glycans were isolated using Sep-Pak C18 columns and subsequently dried using a Speed-Vac. The dried samples were reconstituted in NaOH, and methyl iodide was introduced for a duration of 30 minutes. The glycans were then dehydrated using chloroform and nitrogen gas. They were subsequently dissolved in acetonitrile, combined with 2,5-dihydroxybenzoic acid (in methanol and water), and these mixtures were spotted onto an MTP384 plate and allowed to dry. Mass spectra were acquired utilizing liquid chromatography–mass spectrometry (LC–MS) (Bruker, USA).

2.7. Cell culture and DEHP/MEHP exposure conditions

HCT116 human colorectal cancer cells were obtained from the Food Industry Research and Development Institute. The cells were cultured in McCoy's 5 A medium (Gibco Life Technologies, USA) supplemented with 10 % fetal bovine serum (FBS, GIBCO, USA), 100 units/mL of penicillin, and 100 μg/mL of streptomycin (GIBCO, USA) at 37°C in a 5 % CO2 atmosphere, with passaging every 2–3 days. For long-term exposure to phthalates, 10 μM of DEHP, MEHP, or control (DMSO) were incorporated into a fresh culture medium and maintained with the cells at each passage for a duration of eight weeks (Chen et al., 2018).

2.8. Cell viability assay

After treatment with control, DEHP, or MEHP (10 μM), the cells were seeded (6000 cells/100 μL) into each well of a 96 well-plate and incubated for 24 hours at 37°C and 5 % CO_2. The culture medium was removed, and a fresh culture medium containing 0–8 mg/mL of A50 or I50 was added. After 24 hours of incubation, the medium was removed, and 10 μL of Cell Counting Kit-8 (CCK-8) reagent (APOLO Biochemical, Inc., Taiwan) and 100 μL of fresh medium were added. Following one hour of incubation, absorbance at 450 nm was measured using a spectrophotometer (Agilent Technologies, Inc., USA). The percentage of cell viability was calculated. All experiments were conducted in triplicate.

2.9. Invasion assay

Invasion assay was carried out using transwell inserts with an eight μm pore size (Corning, USA) coated with matrigel (Corning, USA). In brief, the cells were exposed to 10 μM/mL of either control, DEHP, or MEHP for eight weeks. Then, 4×10^5 cells were seeded into the upper insert and incubated at 37 °C with 5 % CO_2. After 24 hours, the cells were fixed with 4 % paraformaldehyde for 30 minutes and stained with crystal violet for 30 minutes. The number of invasive cells was then counted under an optical microscope. All experiments were repeated in triplicate.

2.10. Wound healing assay

We prepared a cell suspension (5×10^5/mL) and added 70 μL to each well insert (ibidi, USA). After 24 hours of incubation, the cell formed a confluent layer. The insert was then removed, and a fresh culture medium supplemented with either control, DEHP, or MEHP (10 μM) was added. The cell-covered areas were captured using a microscope immediately after the insert removal and after another 24 hours of incubation. The migratory areas were measured using ImageJ software and compared between the 0-hour and 24-hour time points. All experiments were conducted in triplicate.

2.11. Sphere-forming assay

The cells (1000 cells/mL) after treatment with either control, DEHP, or MEHP (10 μM) were seeded into the well of ultra-low attachment 24-well plate and cultured in serum-free medium containing Transferrin, B27, insulin, Selenium Solution (ITS-G) (Gicbo Life Technologies, USA), 1 % penicillin-streptomycin (Hyclone, USA), 20 ng/mL of EGF, and 10 ng/mL basic FGF (Gibco Life Technologies, USA) for 7 days at 37°C and 5 % CO_2. The sizes of spheres were then captured and measured using a microscope. All experiments were performed in triplicate.

2.12. Statistical analysis

All data was performed and analyzed using GraphPad Prism 8 software (GraphPad Software, Inc., San Diego, CA). Data were represented as mean ± SD. Differences between the two groups were analyzed using an unpaired Student's t-test unless otherwise stated. Differences compared to three or more than three groups were analyzed using one-way ANOVA followed by the Kruskal–Wallis test. A p-value <0.05 was considered to be statistically significant.

3. Results

3.1. Distinct structures were identified from water- or ethanol-eluted Aloe vera extracted polysaccharides

The *Aloe vera* gel powder was dissolved in deionized water and subjected to HP-20 gel column chromatography. The polysaccharide A50 was eluted with water, while I50 was eluted with ethanol. To determine the acemannan content in A50 and I50, the polysaccharides were separated using HPLC and RID. The chromatogram displayed a peak of acemannan in A50 at 14.384 minutes (Fig. 1**A**) and in I50 at 16.288 minutes (Fig. 1**B**). The acemannan contents for A50 and I50 were found to be 49.77 % and 87.2 %, respectively. Additionally, the polysaccharides were analyzed using UV–Vis spectrometry to evaluate the O-acetyl group content in A50 and I50. The levels of the O-acetyl group were measured at 492.85 mg/g for A50 and 640.64 mg/g for I50 (Table 1).

We further characterized the O-acetyl groups of A50 and I50 by utilizing FT-IR and NMR spectroscopy. The spectra of A50 and I50 displayed peaks at 3295/3435, 1733/1735, 1575/1653, and 1236/1247 cm^{-1}, corresponding to –OH, C═O, COO–, and C–O–C stretching, respectively, confirming the presence of O-acetyl esters (Ni et al., 2004; Rodríguez-González et al., 2011) (Fig. 2**A**). In the ^{1}H NMR spectrum, the O-acetyl groups of A50 and I50 exhibited a characteristic signal between 2.00 and 2.10 ppm, which is considered a fingerprint of *Aloe vera* (Fig. 2**B**). Additionally, signals for methyl groups between 2.03 and 2.13 ppm in the 1H NMR spectrum of I50 suggested the presence of O-acetyl groups at different locations. This was further supported by corresponding methyl carbon signals at 20.5, 20.3, and 20.1 ppm, and carboxyl carbon signals between 172.6 and 173.9 ppm in the ^{13}C NMR spectrum (Fig. 2**C**). Furthermore, sugar rings and anomeric protons appeared in the range of 3.4–5.5 ppm in the ^{1}H NMR spectrum. The ^{13}C NMR spectrum of I50 displayed signals in the anomeric region (98.5–102.5 ppm), indicating the presence of mannopyranose and glucopyranose units. Overall, the ^{1}H and ^{13}C NMR spectra of A50 closely resembled those of I50. ^{1}H NMR, ^{13}C NMR, and FT-IR spectra indicate that both compounds possess structures similar to acemannan (Bozzi et al., 2007; Chokboribal et al., 2015). These findings suggest that the different solvents used for eluting *Aloe vera* polysaccharides lead to variations in acemannan and O-acetyl group contents.

3.2. Aloe vera-extracted polysaccharides reversed phthalate-induced glycosylation alteration in colorectal cancer cells

Evidence indicates that aberrant glycosylation is involved in cancer

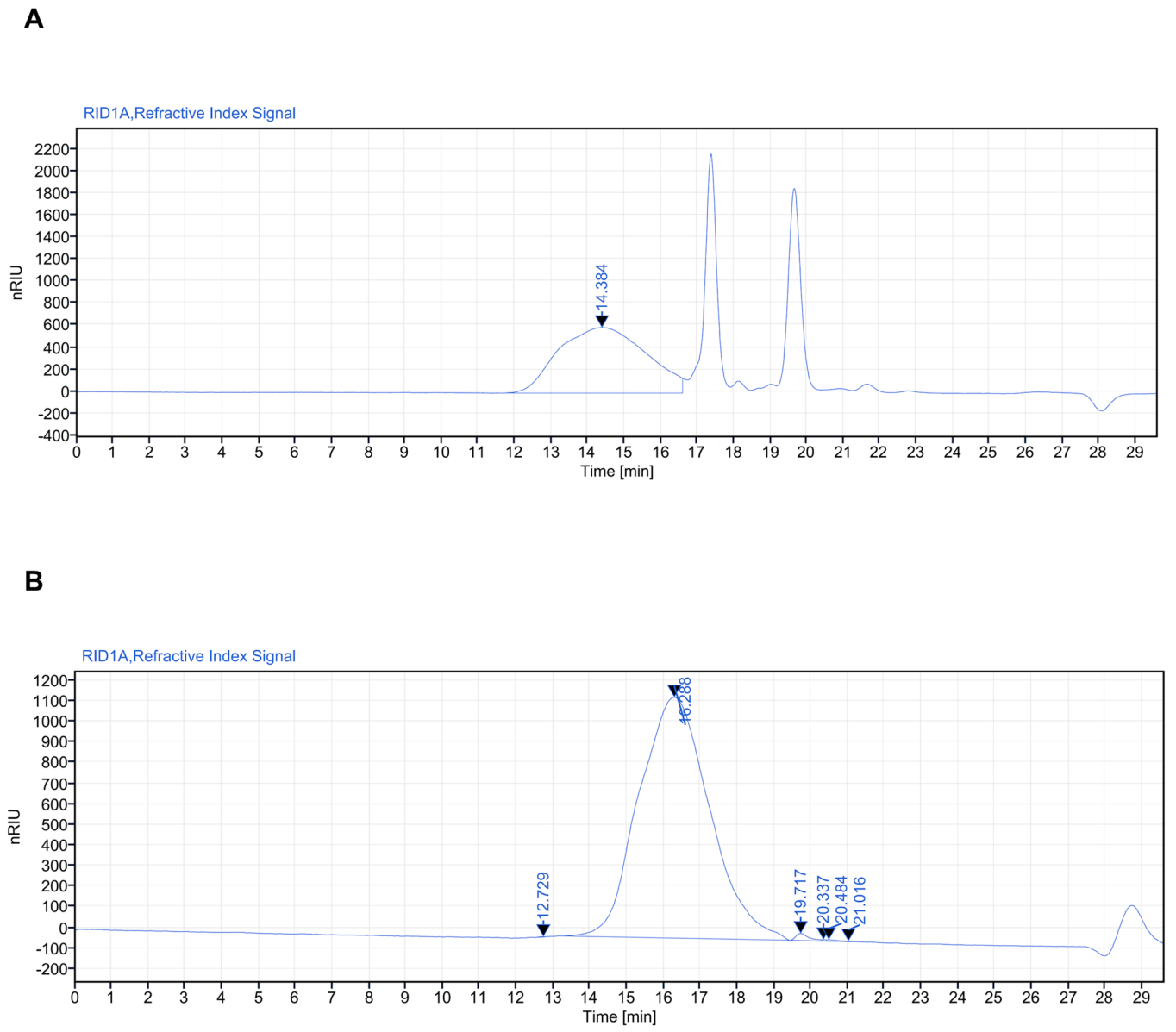

Fig. 1. Analysis of acemannan content in *Aloe vera* polysaccharides A50 and I50. The HPLC spectra of A50 (A) and I50 (B) revealed retention times of 14.384 minutes and 16.288 minutes, respectively.

Table 1
Determination of acemannan and O-acetyl group content of *Aloe vera* polysaccharides, A50 and I50.

Sample	Acemannan content (%)	O-acetyl group content (mg/g)
A50	49.77±0.74	492.85±21.69
I50	87.2±1.53	640.64±12.24

progression and can potentially become a therapeutic target (Chiang et al., 2021; Pinho and Reis, 2015; Thomas et al., 2021). Compounds derived from plants are capable of changing glycan patterns on cells (Cabrera et al., 2012). To investigate whether polysaccharides extracted from *Aloe vera* would change the glycosylation of colorectal cancer cells, we exposed HCT116 cells to DEHP or MEHP for eight weeks. Cell surface glycoproteins were purified, and the *N*-glycome of the glycoproteins was released and analyzed using LC–MS. A total of 37 glycans were examined, and the relative intensities of the predicted glycans are shown in Fig. 3. Most of the glycans remained generally unchanged; however, specific alterations were detected in phthalate-exposed cells. Of particular interest, sialylated and high-mannose *N*-glycan structures, including increases in N2H5, N2H6, N2H7, N2H8, and N4H5S1, as well as decreases in N5H6S3 and N5H6S4, were observed with MEHP exposure. In DEHP-treated HCT116 cells, only N2H3 and N2H5 showed substantial reductions. The phthalate-induced *N*-glycan changes were reversed in the presence of A50 and I50. The complex structure N5H6S3 was reduced by about fivefold under MEHP exposure; however, treatment with A50 or I50 reversed this significant reduction. Similar effects were also observed in other altered glycan structures, such as N2H7, N2H8, and N4H5S1 (Fig. 3**B**, **C**). These results suggest that certain *N*-glycan patterns, including high-mannose and complex forms, vary when colorectal cancer cells are exposed to phthalates; however, *Aloe vera*–extracted compounds can protect against these alterations. Glycosylation-associated malignant phenotypes in colorectal cancer induced by phthalates may be effectively inhibited by A50 and I50 treatment, implying their therapeutic potential.

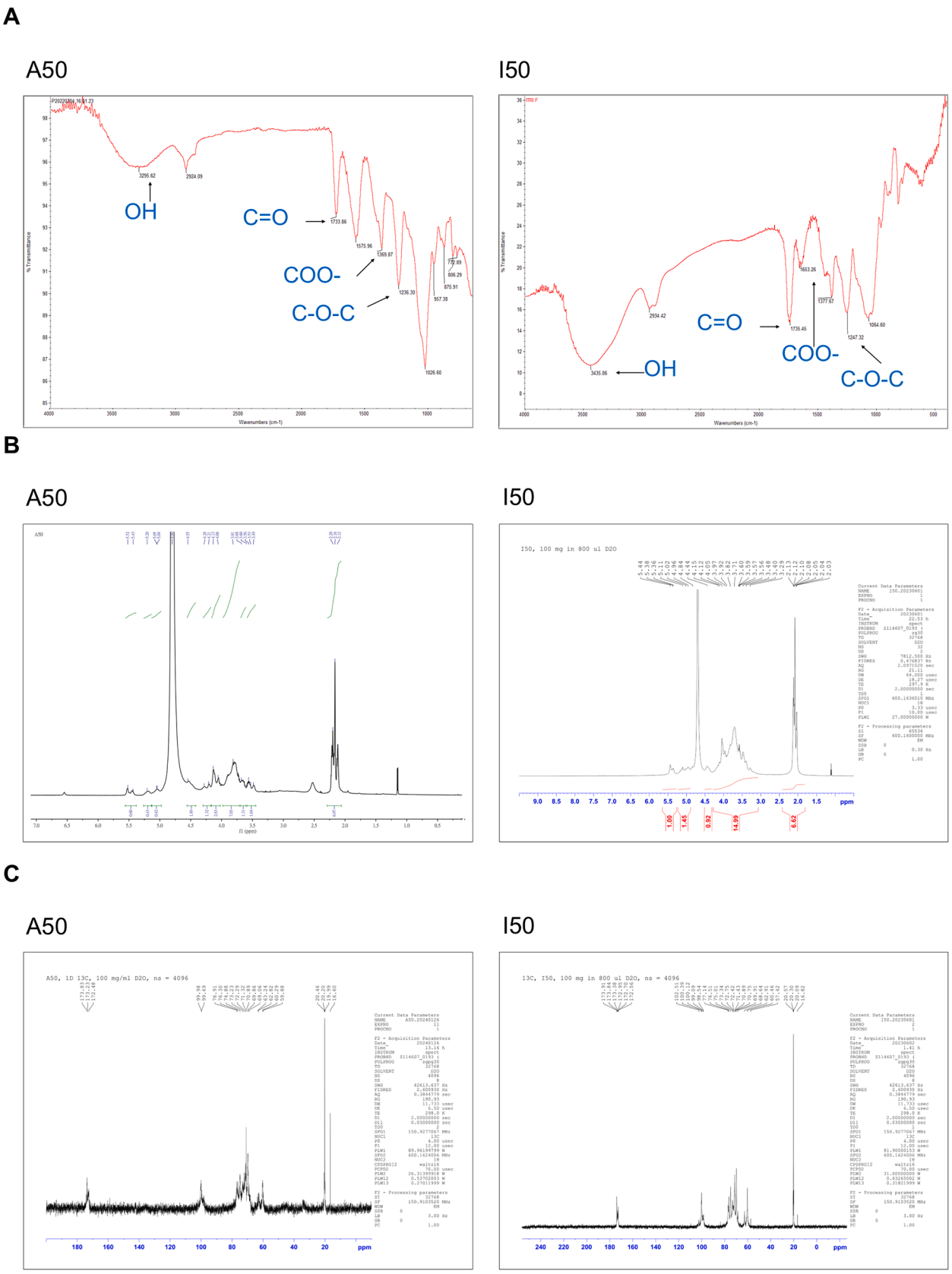

Fig. 2. Characterization of the O-acetyl group and acemannan from *Aloe vera* polysaccharides A50 and I50. The FT-IR spectra (A), ^{1}H NMR spectra (B), and ^{13}C NMR spectra (C) of A50 and I50 are presented.

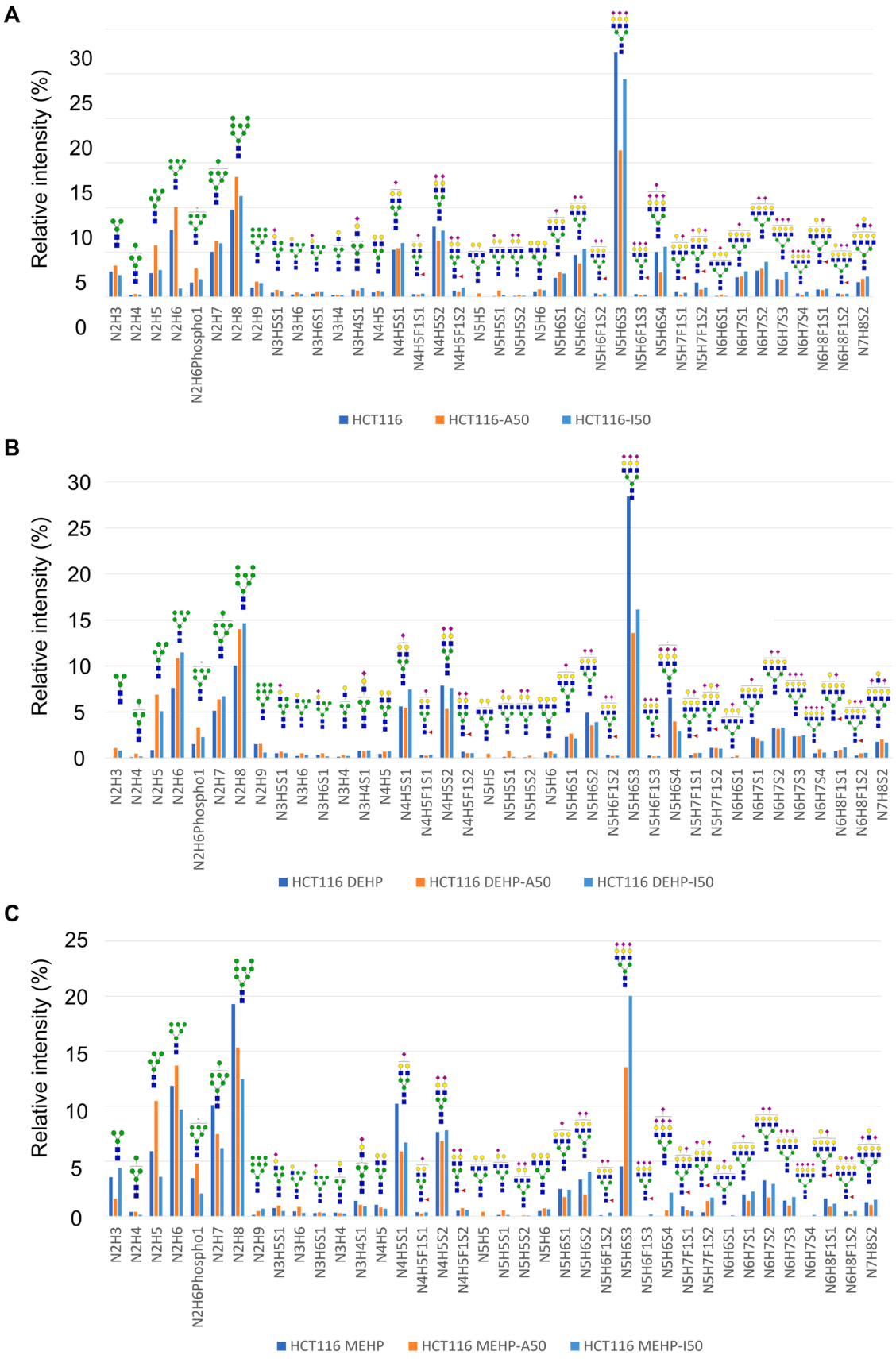

Fig. 3. Effects of A50 and I50 on N-glycan profiles altered by DEHP or MEHP exposure. The N-glycan patterns were determined using LC–MS in HCT116 cells under control conditions (A), 10 μM DEHP exposure (B), and 10 μM MEHP (C) exposure, followed by treatments with A50 (8 mg/mL) or I50 (8 mg/mL). The relative intensities of each glycan signal are presented.

3.3. A50, but not I50, reduced phthalate-induced viability in colorectal cancer cells

Since our findings indicate that *Aloe vera*–extracted polysaccharides treatment modifies the cell surface *N*-glycome of phthalate-treated colorectal cancer cells, we further investigate the functional effects of *Aloe vera*–extracted polysaccharides on colorectal cancer cells. Our previous studies have established a correlation between malignancy and drug resistance in colorectal cancer and long-term exposure to phthalates (Chen et al., 2018; Shih et al., 2023). To ascertain whether *Aloe vera* polysaccharides, specifically A50 and I50, inhibit the protumoral effects of phthalates, we evaluated cancer cell viability following treatment with A50 and I50. HCT116 cells were exposed to DEHP or MEHP in the presence of A50 and I50 at concentrations ranging from 0 to 8 mg/mL, and cell viability was assessed using the CCK-8 assay. A50 significantly reduced cell viability induced by DEHP and MEHP in a dose-dependent manner (Fig. 4**A**). In contrast, I50 exhibited no significant effect on cell viability in HCT116 cells exposed to DEHP or MEHP (Fig. 4**B**).

3.4. A50 and I50 exhibited different properties on phthalate-induced migration of colorectal cancer cells

Phthalate exposure has been shown to upregulate markers of epithelial–mesenchymal transition, including N-cadherin, vimentin, and α-smooth muscle actin expression, while further promoting the migration of HCT116 cells (Chen et al., 2018). Therefore, we investigated whether polysaccharides extracted from *Aloe vera*, specifically A50 and I50, could mitigate the invasion and migration of HCT116 cells under exposure to DEHP or MEHP. HCT116 cells, with or without phthalate exposure, were seeded into the upper chamber of transwell plates coated with Matrigel. We applied a concentration of 8 mg/mL of A50 or I50 based on prior cell viability results for the subsequent treatments. After 24 hours of incubation, the migrated cells in the lower chamber were stained and counted. Both DEHP and MEHP significantly enhanced the invasion of HCT116 cells. A50 markedly reduced the invasion triggered by DEHP, while I50 inhibited the effects of MEHP (Fig. 5**A**, **B**). We also assessed cell migration using a wound-healing assay. Under phthalate exposure, A50 did not affect cell migration; however, I50 significantly inhibited DEHP-induced migration. Furthermore, neither A50 nor I50 influenced the migration of HCT116 cells exposed to MEHP (Fig. 5**C**). Overall, these results demonstrate that compounds extracted from *Aloe vera* exert different effects on the invasion and migration of colorectal cancer cells following phthalate exposure.

3.5. I50, but not A50, inhibited phthalate-induced stemness ability in colorectal cancer cells

Phthalate exposure has been demonstrated to promote colorectal cancer stemness (Chen et al., 2018; Shih et al., 2023). To further examine the effects of A50 and I50 on the stemness of colorectal cancer

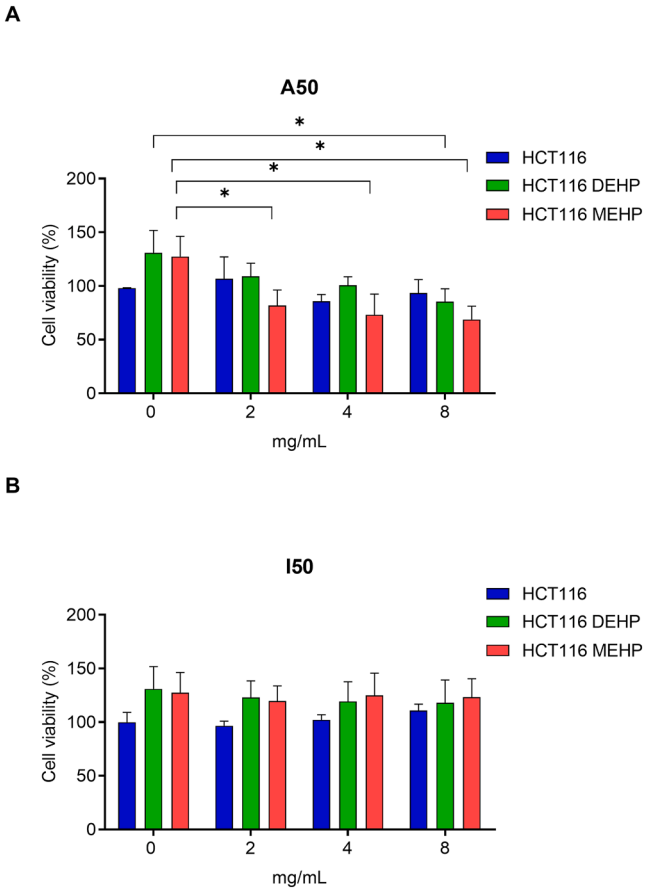

Fig. 4. Effects of A50 and I50 on cell viability induced by DEHP and MEHP. (A) The HCT116 cells were treated with control, DEHP (10 μM), and MEHP (10 μM), followed by treatment with A50 (A) and I50 (B). Cell viability was assessed using the CCK-8 assay. Data are presented as means ± SD from at least three independent experiments. *$P < 0.5$.

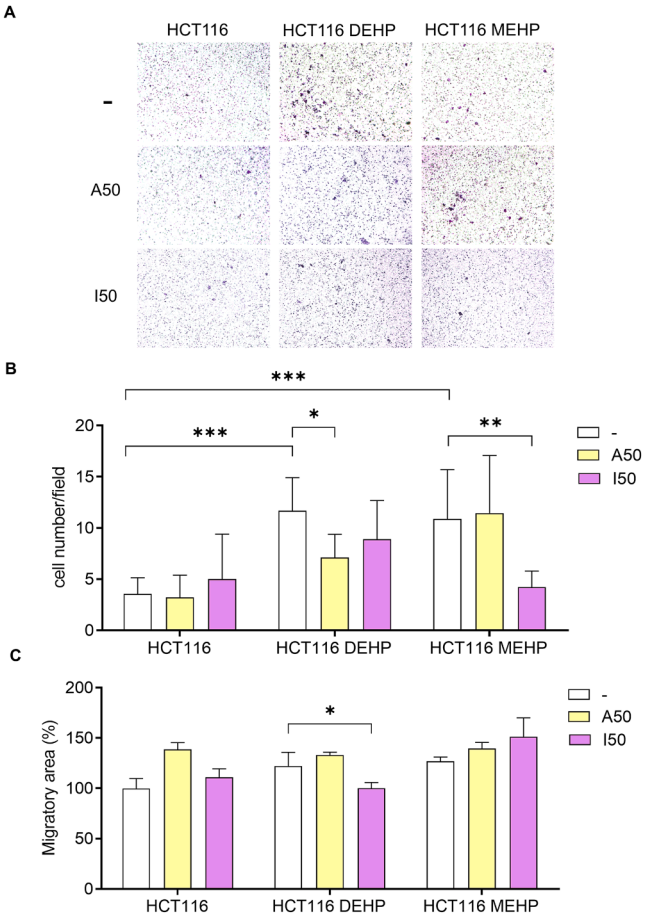

Fig. 5. Effects of A50 and I50 on cell migration induced by DEHP and MEHP. HCT116 cells were treated with control, DEHP (10 μM), and MEHP (10 μM), followed by treatments with A50 (8 mg/mL) and I50 (8 mg/mL). (A, B) A Transwell migration assay was performed. Representative crystal violet staining images (A) and quantification of migrated cells (B) are shown. Original magnification: ×100. Data are presented as means ± SD from at least three independent experiments. *$P < 0.5$, **$P < 0.01$ and ***$P < 0.001$. (C) Statistical results of the wound-healing assay. Data are presented as means ± SD from at least three independent experiments. *$P < 0.5$.

cells, we performed a sphere-forming assay, a three-dimensional culturing method used to assess stemness capabilities. We evaluated the sizes of the spheres in HCT116 cells exposed to DEHP or MEHP, followed by treatment with 8 mg/mL A50 and I50. As illustrated in Fig. 6, DEHP and MEHP significantly enhanced sphere formation. Notably, while A50 did not influence sphere formation following exposure to DEHP or MEHP, I50 demonstrated significant inhibitory effects. These findings suggest that I50 is more effective than A50 in inhibiting phthalate-induced stemness.

4. Discussion

Phthalates are a group of chemical compounds commonly utilized as plasticizers, essential for enhancing the flexibility, durability, and resilience of various industrial and consumer plastic products. Concerns have emerged regarding several phthalates, including DEHP, dibutyl phthalate, and benzyl butyl phthalate, due to their potentially harmful effects, which encompass endocrine disruption, reproductive system abnormalities, developmental problems, as well as carcinogenesis (Heudorf et al., 2007; Hyun Kim et al., 2018; Kay et al., 2013; Lyche et al., 2009; Winz et al., 2023). AhR is the well-studied molecular target of phthalate that induces the cAMP-PKA-CREB1 cascade, leading to breast cancer progression (Hsieh et al., 2022; Mughees et al., 2022). Additionally, phthalates promote cell proliferation by activating the ERK5/p38 pathway in prostate cancer (Zhu et al., 2018). Furthermore, a clinical cohort study has identified a correlation between high phthalate exposure and an increased incidence of prostate cancer (Chuang et al., 2020). Phthalate exposure is considered to elevate cancer risk and facilitate the development of malignant characteristics. However, strategies for treating cancer associated with phthalate exposure remain insufficiently explored.

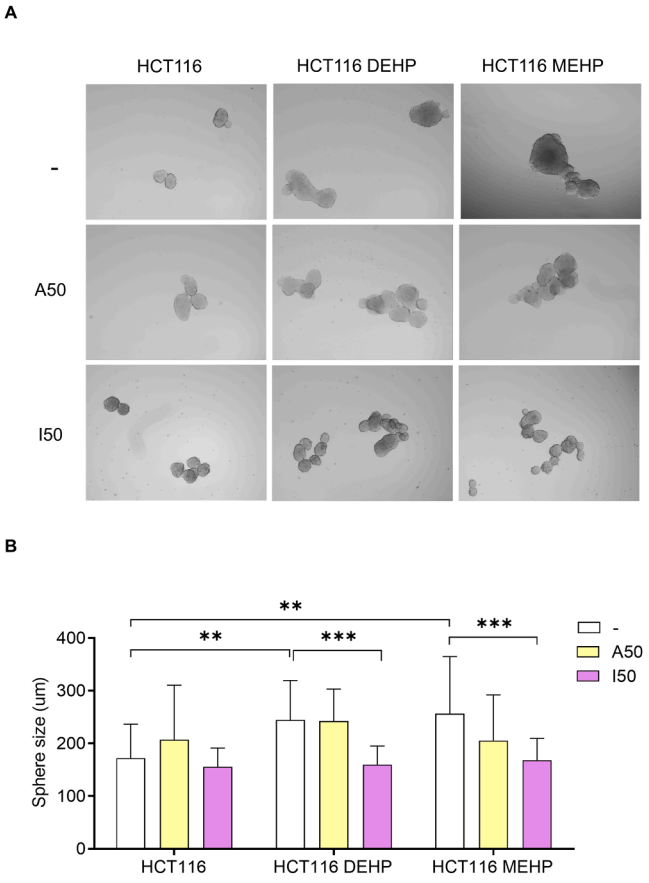

Fig. 6. Effects of A50 and I50 on sphere formation induced by DEHP and MEHP. HCT116 cells were treated with control, DEHP (10 μM), and MEHP (10 μM), followed by treatments with A50 (8 mg/mL) and I50 (8 mg/mL). (A, B) Sphere-forming assays were conducted, with representative bright-field images shown in panel (A) and the quantification results in panel (B). Original magnification: ×200. Data are presented as means ± SD from at least three independent experiments. $^{**}P < 0.01$ and $^{***}P < 0.001$.

MEHP is the primary metabolite of DEHP (Choi et al., 2012). DEHP, which contains the diester group, enters the cell and is hydrolyzed to MEHP, characterized by the monoester group, histidine triad nucleotide–binding protein, and human liver microsomes. Previous research has indicated that DEHP and MEHP exert distinct effects on insulin signaling and glucose transporter four translocation, potentially due to their structural differences. These differences are believed to influence their interaction with unsaturated fatty acids within the plasma membrane, thereby disrupting membrane integrity and fluidity (Viswanathan et al., 2017). However, our results did not reveal significant differences in the phenotypes induced by DEHP- and MEHP-exposed colorectal cancer cells. Interestingly, we did observe variations in N-glycan patterns following exposure to these phthalates, which we speculate may be related to the metabolic processes within the cells. Glycosylation, the process of attaching glycans to proteins or lipids, is influenced by metabolic flux due to its role in energy metabolism. This process primarily involves the hexosamine biosynthetic pathway, a critical route for glucose metabolism. Glycosylation also senses metabolic changes and exhibits aberrant variation to modulate cell functions in cancer (Carvalho-Cruz et al., 2018). In our cell models, HCT116 cells exposed to DEHP require an additional step to convert into MEHP, involving a complex network of processes. The intricate relationship between metabolism and glycosylation, with many pathways still not fully understood, likely accounts for the different glycosylation patterns observed in HCT116 cells treated with DEHP or MEHP.

Our previous study demonstrated that phthalates downregulate the expression of sialyltransferase ST8IA6, which leads to cancer stemness and tumorigenesis (Shih et al., 2023). Glycosylation critically influences normal cellular functions. Changes in glycosylation are identified to be involved in multiple processes in cancer progression (Pinho and Reis, 2015). Long-term exposure to DEHP/MEHP in HCT116 cells resulted in several glycosylation modifications (Fig. 3). Notably, treatment with *Aloe vera* polysaccharides was found to mitigate these changes, a phenomenon not previously reported. The results indicated that alterations in specific *N*-glycan structures can be reversed to varying degrees in the presence of A50 and I50, potentially offering a viable therapeutic approach for addressing malignancies induced by glycosylation changes; however, further investigation into the underlying molecular mechanisms is warranted. Additionally, HCT116 cells treated with DEHP or MEHP exhibited malignant behaviors, including increased cell viability, migration, and stemness (Figs. 4–6). *Aloe vera* polysaccharides mitigated these effects. These findings suggest that *Aloe vera* may play a regulatory role in signal transduction pathways, thereby influencing cellular function.

We obtained A50 and I50 from the elution of *Aloe vera* using water and ethanol, respectively. The primary difference between these polysaccharides is their acemannan and O-acetyl group contents. The O-acetyl group is a crucial structure within acemannan, contributing to its bioactivities (Liu et al., 2019). We evaluated the effects of A50 and I50 on phthalate-induced colorectal cancer cell phenotypes, including cell viability, migration, and stemness, and observed significant differences. This supports the evidence that the O-acetyl group enhances the bioactivity of acemannan. Interestingly, in the analysis of cell viability, A50, which has a lower O-acetyl group content, exhibited a more pronounced reduction in phthalate-induced cell viability compared to I50, which possesses a higher O-acetyl group content. *Chokboribal et al.* reported that the O-acetyl group affects the three-dimensional structure of acemannan by altering its hydrophobicity (Chokboribal et al., 2015), suggesting the differences in O-acetyl group-mediated bioactivities between A50 and I50 possibly due to structure rather than the amount. However, this study did not explore the three-dimensional structures of

A50 and I50, which could be crucial for understanding their distinct activities. Further research is warranted to validate this hypothesis and enhance the application of *Aloe vera* in healthcare.

5. Conclusion

Our study elucidated the potential effects of *Aloe vera*–extracted polysaccharides, A50 and I50, on glycosylation and functions of colorectal cancer cells. We successfully isolated and characterized acemannan and O-acetyl groups from *Aloe vera* polysaccharides using various analytical techniques. Our findings revealed significant differences between A50 and I50, suggesting that these variations contribute to their biological activities. This study provides valuable insights into the therapeutic potential of *Aloe vera*–extracted polysaccharides in the management of colorectal cancer. Future research should focus on elucidating the specific molecular pathways underlying the observed effects and exploring the clinical applications of these compounds in cancer treatment.

Funding

This work was supported by a grant from the National Science and Technology Council, Taipei, Taiwan (NSTC 113-2320-B-006-031).

CRediT authorship contribution statement

Pei-Chun Shih: Writing – review & editing, Writing – original draft, Methodology, Investigation, Formal analysis, Conceptualization. **Chung-Hsien Lin:** Software, Methodology. **Uvarani Chokkalingam:** Methodology. **Ekambaranellore Prakash:** Methodology, Conceptualization. **Ching-Nan Kao:** Methodology. **Chuan-Fa Chang:** Writing – review & editing, Writing – original draft, Conceptualization. **Wei-Ling Lin:** Writing – review & editing, Supervision, Conceptualization.

Declaration of Competing Interest

The authors declare that they have no known competing financial interests or personal relationships that could have appeared to influence the work reported in this paper.

Acknowledgments

We are grateful for support from the Department of Medical Laboratory Science and Biotechnology, National Cheng Kung University, and the insights provided by Dr. Anuma Singh.

Data Availability

Data will be made available on request.

References

Angelini, A., et al., 2011. The effect of the plasticizer diethylhexyl phthalate on transport activity and expression of P-glycoprotein in parental and doxo-resistant human sarcoma cell lines. J. Biol. Regul. Homeost. Agents 25, 203–211.
Balan, B.J., et al., 2014. Oral administration of Aloe vera gel, anti-microbial and anti-inflammatory herbal remedy, stimulates cell-mediated immunity and antibody production in a mouse model. Cent. Eur. J. Immunol. 39, 125–130.
Bernard, L., et al., 2015. Migrability of PVC plasticizers from medical devices into a simulant of infused solutions. Int J. Pharm. 485, 341–347.
Bourdeaux, D., et al., 2016. Analysis of PVC plasticizers in medical devices and infused solutions by GC-MS. J. Pharm. Biomed. Anal. 118, 206–213.
Bozzi, A.P., C., Austin, S., Arce Vera, F., 2007. Quality and authenticity of commercial Aloe vera gel powders, 103, 9.
Cabrera, P.V., et al., 2012. High throughput screening for compounds that alter muscle cell glycosylation identifies new role for N-glycans in regulating sarcolemmal protein abundance and laminin binding. J. Biol. Chem. 287, 22759–22770.
Carvalho-Cruz, P., et al., 2018. Cellular glycosylation senses metabolic changes and modulates cell plasticity during epithelial to mesenchymal transition. Dev. Dyn. 247, 481–491.
Chen, H.P., et al., 2018. Phthalate exposure promotes chemotherapeutic drug resistance in colon cancer cells. Oncotarget 9, 13167–13180.
Chiang, A.W.T., et al., 2021. Systems glycobiology for discovering drug targets, biomarkers, and rational designs for glyco-immunotherapy. J. Biomed. Sci. 28, 50.
Choi, K., et al., 2012. In vitro metabolism of di(2-ethylhexyl) phthalate (DEHP) by various tissues and cytochrome P450s of human and rat. Toxicol. Vitr. 26, 315–322.
Chokboribal, J., et al., 2015. Deacetylation affects the physical properties and bioactivity of acemannan, an extracted polysaccharide from Aloe vera. Carbohydr. Polym. 133, 556–566.
Chuang, S.C., et al., 2020. Phthalate exposure and prostate cancer in a population-based nested case-control study. Environ. Res 181, 108902.
Fatma Salah, Y.E.G., Abdelkarim, Mahdhi, Hatem, Majdoub, Nathalie, Jarroux, Faouzi, Sakli, 2017. Effect of the deacetylation degree on the antibacterial and antibiofilm activity of acemannan from Aloe vera. Ind. Crops Prod. 103, 6.
Govindarajan, S., et al., 2021. Aloe vera carbohydrates regulate glucose metabolism through improved glycogen synthesis and downregulation of hepatic gluconeogenesis in diabetic rats. J. Ethnopharmacol. 281, 114556.
Hekmatpou, D., et al., 2019. The Effect of Aloe vera Clinical Trials on Prevention and Healing of Skin Wound: A Systematic Review. Iran. J. Med Sci. 44, 1–9.
Heudorf, U., et al., 2007. Phthalates: toxicology and exposure. Int J. Hyg. Environ. Health 210, 623–634.
Hsieh, T.H., et al., 2022. DEHP mediates drug resistance by directly targeting AhR in human breast cancer. Biomed. Pharm. 145, 112400.
Hyun Kim, D., et al., 2018. Risk assessment of endocrine disrupting phthalates and hormonal alterations in children and adolescents. J. Toxicol. Environ. Health A 81, 1150–1164.
Jadhao, M., et al., 2021. The long-term DEHP exposure confers multidrug resistance of triple-negative breast cancer cells through abc transporters and intracellular ROS. Antioxid. (Basel) 10.
Kay, V.R., et al., 2013. Reproductive and developmental effects of phthalate diesters in females. Crit. Rev. Toxicol. 43, 200–219.
Khan, T., Cabral, H., 2021. Abnormal glycosylation of cancer stem cells and targeting strategies. Front Oncol. 11, 649338.
Kumar, S., Kumar, R., 2019. Role of acemannan O-acetyl group in murine radioprotection. Carbohydr. Polym. 207, 460–470.
Liu, C., et al., 2019. Extraction, Purification, structural characteristics, biological activities and pharmacological applications of acemannan, a polysaccharide from aloe vera: a review. Molecules 24.
Lyche, J.L., et al., 2009. Reproductive and developmental toxicity of phthalates. J. Toxicol. Environ. Health B Crit. Rev. 12, 225–249.
Maan, A.A., et al., 2018. The therapeutic properties and applications of Aloe vera: A review. J. Herb. Med. 12, 1–10.
Manirakiza, A., et al., 2021. Aloe and its effects on cancer: a narrative literature review. East Afr. Health Res J. 5, 1–16.
Mariana, M., et al., 2023. Phthalates' exposure leads to an increasing concern on cardiovascular health. J. Hazard Mater. 457, 131680.
Metcalfe, C., 2019. Quantitation of aloe vera polysaccharides by o-acetyl and uv-vis spectrophotometry: first action 2018.14. J. AOAC Int 102, 1091–1094.
Minjares-Fuentes, R., et al., 2017. Effect of different drying procedures on the bioactive polysaccharide acemannan from Aloe vera (Aloe barbadensis Miller). Carbohydr. Polym. 168, 327–336.
Minjares-Fuentes, R., et al., 2018. Compositional and structural features of the main bioactive polysaccharides present in the aloe vera plant. J. AOAC Int 101, 1711–1719.
Mughees, M., et al., 2022. Mechanism of phthalate esters in the progression and development of breast cancer. Drug Chem. Toxicol. 45, 1021–1025.
Murtazina, A., et al., 2022. Anti-cancerous potential of polysaccharides derived from wheat cell culture. Pharmaceutics 14.
Nejatzadeh-Barandozi, F., 2013. Antibacterial activities and antioxidant capacity of Aloe vera. Org. Med Chem. Lett. 3, 5.
Nejatzadeh-Barandozi, F., Enferadi, S.T., 2012. FT-IR study of the polysaccharides isolated from the skin juice, gel juice, and flower of Aloe vera tissues affected by fertilizer treatment. Org. Med Chem. Lett. 2, 33.
Ni, Y., et al., 2004. Isolation and characterization of structural components of Aloe vera L. leaf pulp. Int Immunopharmacol. 4, 1745–1755.
Pinho, S.S., Reis, C.A., 2015. Glycosylation in cancer: mechanisms and clinical implications. Nat. Rev. Cancer 15, 540–555.
Rodríguez-González, V.M., F, A., González-Laredo, R.F., Rocha-Guzmán, N.E., Gallegos-Infante, J.A., Candelas-Cadillo, M.G., Ramírez-Baca, P., Simal, S., Rosselló, C., 2011. Effects of pasteurization on bioactive polysaccharide acemannan and cell wall polymers from Aloe barbadensis miller. Carbohydr. Polym. 86, 9.
Shi, X.D., et al., 2018. Structural and conformational characterization of linear O-acetyl-glucomannan purified from gel of aloe barbadensis miller. Int J. Biol. Macromol. 120, 2373–2380.
Shih, P.C., et al., 2023. Long-term DEHP/MEHP exposure promotes colorectal cancer stemness associated with glycosylation alterations. Environ. Pollut. 327, 121476.
Siegel, R.L., et al., 2023. Colorectal cancer statistics, 2023. CA Cancer J. Clin. 73, 233–254.
Tai-Nin Chow, J., et al., 2005. Chemical characterization of the immunomodulating polysaccharide of Aloe vera L. Carbohydr. Res 340, 1131–1142.
Takeshita, A., et al., 2006. The endocrine disrupting chemical, diethylhexyl phthalate, activates MDR1 gene expression in human colon cancer LS174T cells. J. Endocrinol. 190, 897–902.
Thomas, D., et al., 2021. Altered glycosylation in cancer: a promising target for biomarkers and therapeutics. Biochim Biophys. Acta Rev. Cancer 1875, 188464.

Very, N., et al., 2018. Drug resistance related to aberrant glycosylation in colorectal cancer. Oncotarget 9, 1380–1402.
Viswanathan, M.P., et al., 2017. Effects of DEHP and its metabolite MEHP on insulin signalling and proteins involved in GLUT4 translocation in cultured L6 myotubes. Toxicology 386, 60–71.
Wang, A., et al., 2023. Dietary plant polysaccharides for cancer prevention: role of immune cells and gut microbiota, challenges and perspectives. Nutrients 15.
Winz, C., et al., 2023. Endocrine-disrupting compounds and metabolomic reprogramming in breast cancer. J. Biochem Mol. Toxicol. 37, e23506.
Zhang, Y., et al., 2022. Health risks of phthalates: a review of immunotoxicity. Environ. Pollut. 313, 120173.
Zhu, M., et al., 2018. Phthalates promote prostate cancer cell proliferation through activation of ERK5 and p38. Environ. Toxicol. Pharm. 63, 29–33.